Failure modes and capacity evaluation of Ferro-cement laminated masonry infilled RC frame
Part 2: Proposal and validation of capacity evaluation

Keywords
Masonry infill
Seismic strengthening
Failure modes
Ferro-cement
Infilled RC frame

○Debasish Sen *1
Zasiah Tafheem *1
Matsutaro Seki *4
Md. Shafiul Islam *2
Hamood Alwashali *3
Masaki Maeda*5

1. Introduction

Part 2 intends to evaluate the failure modes identified in Part 1. This is followed by verification of predicted capacities for FC laminated masonry infilled RC frame based on experimental results discussed in Part 1.

2. Lateral strength evaluation

In a particular structural system, the applied load can transfer in different ways, however the structural system fails in a manner that associated with weakest load transfer mechanism. Therefore, the lateral strength of FC strengthened masonry infilled RC frame can be taken as the minimum of calculated lateral capacity of four distinct failure mechanisms (identified in Part-1 of this article) as per Eq. 1.

$$\text{Predicted lateral strength, } Q_{calc.} = \min(Q_1, Q_2, Q_3 \text{ and } Q_4) \quad (1)$$

where, Q_1, Q_2, Q_3, Q_4 = calculated lateral capacities at overall flexural failure; column punching and top joint sliding failure; diagonal compression failure, and diagonal cracking failure, respectively.

2.1 Failure I: Overall flexural

The lateral capacity at overall flexural failure (Q_1), as shown in Figure 1(a), of the FC laminated masonry infilled RC frame has been computed considering the frame as a cantilever, using Eq. 2 and Eq. 3.

$$Q_1 = {}^{M_u}/_{h_o} \quad (2)$$

$$M_u = a_t f_y l_c + 0.5 N l_c \quad (3)$$

where, M_u = moment capacity, a_t = steel area of column main reinforcements, f_y = yield strength of column main reinforcement, l_c = c/c distance of boundary columns, N = axial load on RC columns = $2N'$.

2.2 Failure II: Column punching and top joint sliding

The total shear capacity (Q_2) can be evaluated by Eq. 4 in reference to Figure 1(b).

$$Q_2 = {}_{ps}Q_c + {}_{js}Q_w + {}_{f}Q_c \quad (4)$$

where, ${}_{ps}Q_c$, ${}_{f}Q_c$ = punching shear and flexural shear capacity column, respectively, which is computed as per JBDPA 2001[9]. On the other hand, joint shear capacity (${}_{js}Q_w$) depends on bond between interfaces and is evaluated from Eq. 5.

$${}_{js}Q_w = \tau_{mas} l_w t_{mas} + \tau_{mor,FC} l_w n_s t_{FC} \quad (5)$$

τ_{mas}, $\tau_{mor,FC}$ = bond strength (cohesion) of mortar in masonry joint and ferro-cement; t_{mas}, t_{FC} = thickness of masonry and FC coating; and n_s = number of FC surface. The bond capacity of mortar, for both masonry joint and FC layer, is considered as $0.17\sqrt{f_{mor}}$, (f_{mor} = compressive strength of mortar).

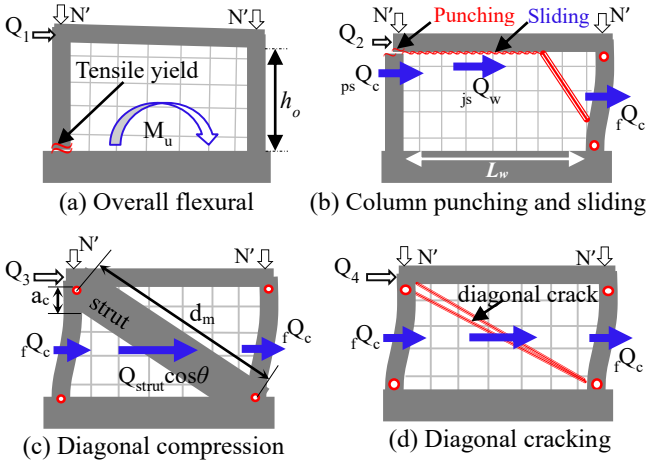

Figure1: Schematic diagram of (a) Failure I, (b) Failure II, (c) Failure III, and (d) Failure IV

2.3 Failure III: Diagonal compression

In this failure, infilled panel (masonry and FC layer) is considered to behave similar to a diagonal strut, as shown in Figure 1(c), that would fail in compression. In addition, flexural hinges would form at the top and bottom of surrounding RC columns. The lateral strength (Q_3) can be evaluated by using Eq. 6.

$$Q_3 = 2\ {}_{f}Q_c + \left(0.5 f_{m,90} W_s t_{mas} + 0.5 f_{mor,FC} W_s n_s t_{FC}\right) cos\theta \quad (6)$$

where, $f_{m,90}$ = expected prism compressive strength of masonry in diagonal direction (= 0.5 × masonry prism compressive strength, f_m); $f_{mor,FC}$ = FC mortar compressive strength; and θ = inclination of compression diagonal with horizontal. The width of the FC laminated masonry (W_s) is considered as Eq. 7, where a_c = contact length. The contact length (a_c) of diagonal strut is calculated by Eq. 8 considering relative stiffness ($\lambda_{mas\text{-}FC}$) of the RC frame and infill panel (masonry and FC coating) that has been proposed by author elsewhere [10].

$$W_s = 2 a_c cos\theta \quad (7)$$

$$a_c = \frac{\pi}{4\lambda_{mas-FC}} \quad (8)$$

$$\lambda_{mas-FC} = \sqrt[4]{\frac{(E_{mas} t_{mas} + E_{FC} n_s t_{FC})\ cos^2\theta}{4 E_C I_c d_m}} \quad (9)$$

where, E_c, E_{mas}, E_{FC} = Young's modulus of concrete, masonry, and FC mortar, respectively; and I_c = moment of inertia of RC column.

フェローセメントにより補強した組積造壁を有する既存 RC 骨組の破壊モードと性能評価
その 2　構造性能の評価法の提案と検証

モハメド　シャフィウル　イスラム、デバシシュ　セン、ザシア　タフィーン、ハムッド　アルワシャリ、関松太郎、前田匡樹

2.4 Failure IV: Diagonal cracking

In this case, a major diagonal crack might appear on the compression diagonal of FC laminated masonry, whereas flexural hinges might form at the ends of columns as shown in Figure 1(d). The lateral capacity is evaluated by Eq. 10.

$$Q_4 = 2\,{}_fQ_c + Q_{mas,cr} + Q_{FC,wm} \quad (10)$$

In this case, contribution of infill masonry ($Q_{mas,cr}$) is considered as the horizontal component of masonry diagonal cracking capacity, in reference to Figure 2 (a), using Eq. 11. The cracking strength of masonry ($f_{mas,cr}$) is considered as $0.05f_m$ as proposed by author elsewhere [11]. The contribution of ferro-cement has been considered to be equal to shear capacity provided by the horizontal mesh reinforcements using Eq. 12 in reference to Figure 2(b). However, an empirical reduction factor (α) has been imposed in the contribution of wire mesh, in Eq. 12, to accommodate less effectiveness of mesh reinforcement compared to contribution in RC shear wall. The less effectiveness might happen because wires are not embedded in RC frame as in shear wall. In this study, the empirical reduction factor (α) has been considered as 0.7 for ferro-cement lamination as proposed by Sen et al. [12].

$$Q_{mas,cr} = f_{mas,cr} d_m t_{mas} \sin\theta \quad (11)$$

$$Q_{FC,wm} = \alpha n_s n_L \left(\frac{h_0}{s}\right) A_s f_{y,wm} \quad (12)$$

where, n_L = number of wire mesh layer; s = spacing of wire mesh; A_s = area of horizontal wire; and $f_{y,wm}$ = yield strength of wire mesh.

3. Validation of lateral strength evaluation

3.1 Confirmation of capacity model for each failure mechanism

In Figure 3(a)-(d), calculated capacities of possible failure mechanisms are shown for particular four specimens (IM-FC-2, IM-FC-3, Sp-5 [1], and S5-FM-FC [2]) which have four distinct failure mechanisms I, II, III and IV, respectively. The calculated capacities of the observed failure mechanism are marked with asterisk (*) sign in Figure 3(a)-(d). The ratio of calculated to experimental capacities are 0.83, 0.88, 0.71 and 0.91 for failure I (flexural), II (Punching), III (diagonal compression) and IV (diagonal cracking), respectively. Therefore, it can be concluded that the proposed lateral capacity model for each failure mechanism works well to compute corresponding lateral capacity.

3.2 Confirmation of lateral capacity evaluation process

In general, the failure mechanism should be governed by minimum calculated lateral capacity of possible failure mechanisms. However, in some particular cases (i.e. specimen IM-FC-2 and IM-FC-3) the minimum lateral capacity is not the governing one. For specimen IM-FC-2, the lateral capacities for flexural, punching and diagonal cracking failure are very close to each other. On the other hand, in specimen IM-FC-3, initially a minor diagonal crack formed at small lateral story drift as discussed in Part-1, however, at higher drift punching failure occurred.

To check accuracy of the evaluation method, calculated flexural capacity (Q_{mu} = capacity of failure I) and shear capacity (Q_{su} = min.

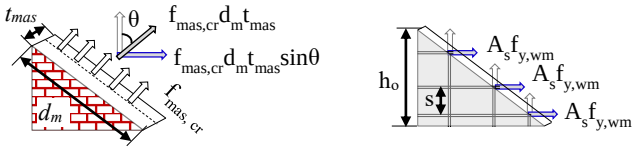

(a) Masonry at cracking (b) Ferro-cement layer at cracking

Figure 2: Schematic diagram of FC laminated masonry at cracking

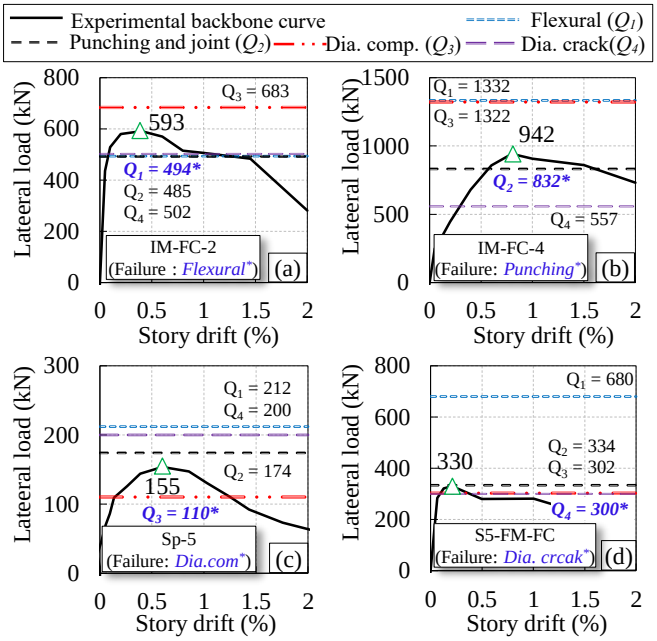

Figure 3: Calculated and experimental capacities (in kN) of (a) IM-FC-2 (b) IM-FC-4, (c) Sp-5 [1] and (d) S5-FM-FC [2] (* observed failure mode)

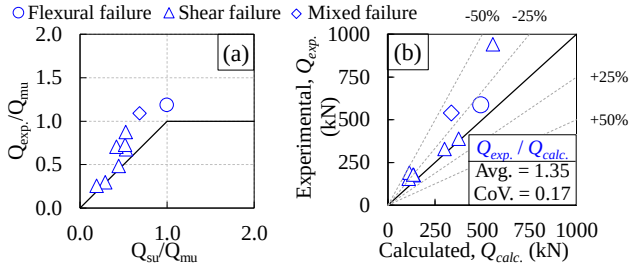

Figure 4: Comparison of calculated and experimental strengths

of shear type failure capacities i.e. II, III and IV) of all available specimens, in the current study and past literature, are compared with experimental capacities in Figure 4(a) which indicates that the prediction method can identify shear and flexural failure properly. In addition, the calculated capacity (minimum of Q_1, Q_2, Q_3 and Q_4) is plotted in Figure 4(b) which indicates a safe prediction, having average experimental to calculated capacity ratio of 1.35.

4. Conclusions

Lateral capacity evaluation method of ferro-cement laminated masonry infilled RC frame is proposed and validated with current and past experimental results.

ACKNOWLEDGMENT

This research is supported by SATREPS project lead by Prof. Nakano Yoshiaki, U. Tokyo and JSPS KAKENHI JP18H01578 (Principal investigator: Prof. Masaki Maeda, Tohoku U.). This work is also supported by JST Program on OPERA project and JSPS KAKENHI JP19K15070 (Principal investigator: Hamood Alwashali, Tohoku U.)

References (continued from Part 1)

[9] Japan Building Digester Prevention Association (JBDPA) standard, 2001.
[10] Sen et al. (2020a), Experimental investigation and capacity evaluation of ferro-cement laminated masonry infilled RC frame17th WCEE.
[11] Sen et al. (2020b), Experimental study on ferro-cement retrofit for RC frame with infilled brick masonry wall 17th WCEE.
[12] Sen et al. (2020c), Investigation of the lateral capacity of ferro-cement retrofitted infilled masonry in RC frame and simplified prediction approach AIJ J. of Tech. and Design, 26(62).

1*東北大学大学院　大学院生
2*東北大学大学院　学術研究員・博士　（工学）
3*東北大学大学院　助教・博士（工学）
4*建築研究所　特別客員研究員・工学博士
5*東北大学大学院研究科　教授　・博士（工学）

1* Graduate student, Graduate School of Engineering, Tohoku University
2* Research Fellow, Graduate School. of Engg. Tohoku University, Ph.D.
3* Asst. Prof, Graduate School of Engineering, Tohoku University, Ph.D.
4* Visiting Research Fellow, Building Research Institute, Dr.Eng
5* Professor, Graduate School of Engineering, Tohoku University, Ph.D.